Published in Palaeogeography, Palaeoclimatology, Palaeoecology 233, issues 3-4, 204-224, 2006
which should be used for any reference to this work

Regional trends in clay mineral fluxes to the Queensland margin and ties to middle Miocene global cooling

Cédric M. John [a,*], Thierry Adatte [b], Maria Mutti [a]

[a] *University of Potsdam, Department of Geosciences, P.O. Box 601553, 14415 Potsdam, Germany*
[b] *Institut de Géologie, 11 Rue Emile Argand, 2007 Neuchâtel, Switzerland*

Abstract

Three ODP sites located on the Marion Plateau, Northeast Australian margin, were investigated for clay mineral and bulk mineralogy changes through the early to middle Miocene. Kaolinite to smectite (K/S) ratios, as well as mass accumulation rates of clays, point to a marked decrease in accumulation of smectite associated with an increase in accumulation of kaolinite starting at ~15.6 Ma, followed by a second increase in accumulation of kaolinite at ~13.2 Ma. Both of these increases are correlative to an increase in the calcite to detritus ratio. Comparison of our record with published precipitation proxies from continental Queensland indicates that increases in kaolinite did not correspond to more intense tropical-humid conditions, but instead to periods of greater aridity. Three mechanisms are explored to explain the temporal trends in clay on the Marion Plateau: sea-level changes, changes in oceanic currents, and denudation of the Australian continent followed by reworking and eolian transport of clays. Though low mass accumulation rates of kaolinite are compatible with a possible contribution of eolian material after 14 Ma, when Australia became more arid, the lateral distribution of kaolinite along slope indicates mainly fluvial input for all clays and thus rules out this mechanism as well as oceanic current transport as the main controls behind clay accumulation on the plateau. We propose a model explaining the good correlation between long-term sea-level fall, decrease in smectite accumulation, increase in kaolinite accumulation and increase in carbonate input to the distal slope locations. We hypothesize that during low sea level and thus periods of drier continental climate in Queensland, early Miocene kaolinite-rich lacustrine deposits were being reworked, and that the progradation of the heterozoan carbonate platforms towards the basin center favored input of carbonate to the distal slope sites. The major find of our study is that increase kaolinite fluxes on the Queensland margin during the early and middle Miocene did not reflect the establishment of a tropical climate, and this stresses that care must be taken when reconstructing Australian climate based on deep-sea clay records alone.

Keywords: Clay minerals; Weathering; Climate fluctuation; Eustasy; Continental margin; Australia; ODP Leg 194

1. Introduction

Climate change impacts continental weathering rates and runoff, which in turn influences soil formation and transport of terrigenous material to the shelf. As the end product of continental weathering processes, detritic clay minerals are key to understanding past changes in weathering regime (Chamley, 1989, 1998; Thiry, 2000; Adatte et al., 2002). When reworked, clay minerals are also indicative of changes in the rate of continental erosion, and can thus potentially reveal feedbacks between the vegetation cover, the

* Corresponding author. Present address: Department of Earth Sciences, University of California, Santa Cruz, CA 95064, USA.
E-mail address: cjohn@pmc.ucsc.edu (C.M. John).

hydrological cycle, and climate. The long-term trend in Cenozoic climate is characterized by a shift from the warm and equable early Eocene period towards colder, more extensively glaciated periods culminating with the Northern Hemisphere glaciations in the Plio-Pleistocene. In the middle Miocene, three rapid (<1 Ma) and pronounced steps in climate cooling lead to the growth of the East Antarctic ice sheet (Kennett, 1985; Flower and Kennett, 1993; Zachos et al., 2001). The middle Miocene episode is one of the most significant of the Neogene because it induced a shift in the strength and turnover rate of oceanic current (Kennett, 1985), as well as one of the largest sea-level fall of the Cenozoic (Haq et al., 1987; Isern et al., 2002; John et al., 2004). Climatic scenarios to explain the middle Miocene climatic event are complex and involve numerous positive and negative feedbacks between the ocean, the atmosphere and the sedimentary reservoirs (Kennett, 1985; Vincent and Berger, 1985; Jacobs et al., 1996). Continental feedbacks during this period are also important, as a link between the hydrological cycle, continental weathering, and climate has often been hypothesized (Raymo, 1994; Föllmi, 1996; Derry and France-Lanord, 1997; Hay et al., 2002).

The goal of this paper is to explore the relationship between clay accumulation, continental weathering and the middle Miocene climate cooling in Northeastern Queensland, Australia. We present new bulk-rock and clay mineral data from the Marion Plateau, and the main question addressed is whether changes in precipitation and temperature on the continent (i.e. primary change in the weathering regime) lead to accumulation of different clay assemblages on the margin, or whether events associated with middle Miocene cooling (such as sea-level fall, changes in vegetation, paleoceanographic changes, etc.) affected reworking and sorting of clays. Continental shelf records are particularly useful archives because they are generally more complete than their terrestrial counterparts, and because they contain inherited terrigenous clay minerals. The choice of the Queensland margin was motivated by the fact that Australia has essentially been a tectonically stable continent since the Cretaceous (Davies et al., 1989; Struckmeyer and Symonds, 1997). Hence, Miocene clay mineral assemblages on this margin will not be affected by tectonic processes, but will result from the interplay of soil formation, reworking of soil horizons and ancient sediments, and from mechanisms associated with sea-level and oceanographic changes.

2. Sample locations, age models, and analytical methods

2.1. Sample locations

The Marion Plateau is located on the Queensland margin, offshore Townsville, Australia (Fig. 1). Several carbonate platforms were deposited on the plateau during the Miocene (see Fig. 1, Shipboard Scientific Party, 2002). The two largest edifices were designated as Northern Marion Platform (hereafter "NMP") and Southern Marion Platform (hereafter "SMP", after Isern et al., 2002, see Fig. 1). ODP Sites 1194, 1192 and 1195 are located on a transect going from the upper carbonate slope to the lower carbonate slope of the NMP. Site 1194 is located in a proximal location at the foot of the NMP at a paleo water-depth of 100–150 m during most of the Miocene (Isern et al., 2002, Fig. 1). Sites 1192 and 1195 are more distal slope sites, with estimated middle Miocene water-depth of 200 m (Isern et al., 2002, Fig. 1). For consistency throughout this paper, sites are always cited in a proximal to distal order (i.e. Sites 1194, 1192 and 1195), and stratigraphic depths are given in meters below sea-floor (mbsf). We used the shipboard age-models (Isern et al., 2002) to select sampling intervals for lower to lower upper Miocene sediments (from 18 to 10 Ma). We consequently sampled every 0.5 m between 100 and 310 mbsf at Holes 1194A and 1194B, between 210 and 340 mbsf at Hole 1192B, and between 200 and 420 mbsf at Hole 1195B. Because sediment recovery was variable, some site could not be evenly sampled. Site 1194 in particular has many gaps in the recovery and the sampling density is lower than at other sites. Site 1195 on the other hand is the most complete section available, whereas Site 1192 has intermediate recovery. The total number of samples taken for this study was 491: 74 samples from Site 1194 (holes A and B), 140 samples from ODP Hole 1192B, and 277 samples from ODP Hole 1195B (Fig. 1).

2.2. Age models

The age models used in this paper are based on the shipboard age models (Isern et al., 2002), with minor corrections based on the stable isotope stratigraphy as described in John and Mutti (2005). Hence, the age models are based on a combination of magnetostratigraphy, biostratigraphy (nannofossils and planktonic foraminifers datums) and chemostratrigraphy (mainly used to control the age model). Age uncertainties vary between sections. Site 1194 (holes A and B) is richer in neritic carbonates, is more extensively altered by dia-

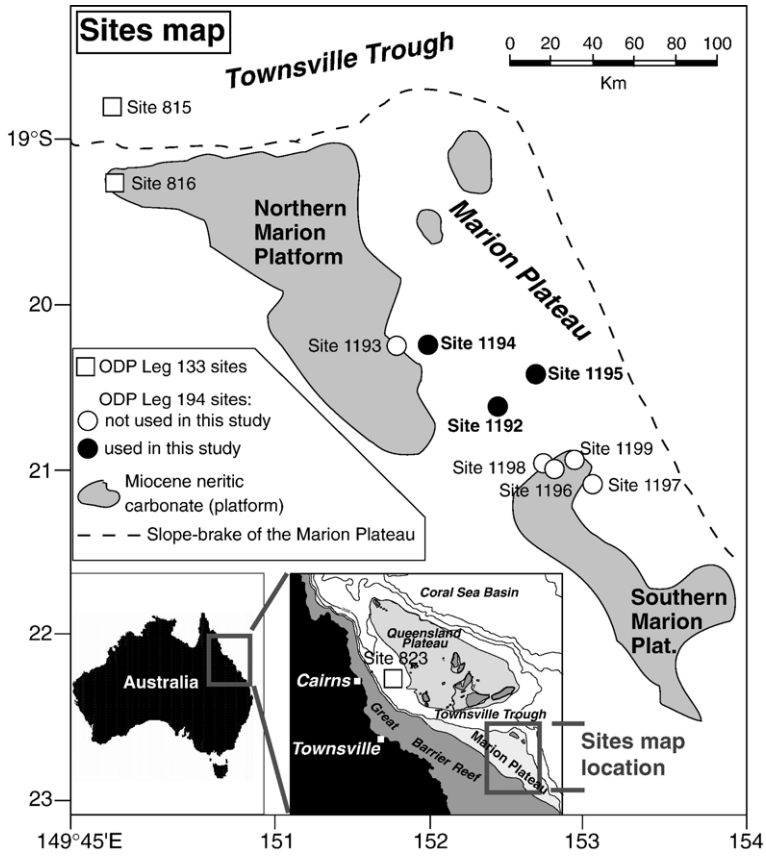

Fig. 1. Location of the sites investigated during this study. Location of the sites drilled during Leg 133 are also indicated. Modified from John (2003).

genesis, and biostratigraphic controls are scarce; age uncertainty is estimated to be ± 1.0 my at this site (John and Mutti, 2005). Dolomitization in the lower interval at Hole 1192B and inconsistencies between magnetostratography, nannofossil and planktonic foraminifers datums in the middle interval of this site give an age uncertainty between ± 0.5 to ± 1.0 my. In contrast, Hole 1195B was drilled as a reference site for biostratigraphy (Isern et al., 2002). Biostratigraphic datums, magnetostratigraphy and stable isotope markers are abundant and correlate well at this site, and age uncertainty was estimated to be ± 0.5 my or better (John and Mutti, 2005). Uncertainties in the age model of Site 1195 were shown to not significantly affect patterns in mass accumulation rates (John and Mutti, 2005). Consequently, this section is used as a reference site throughout this paper.

2.3. Analytical methods

All analyses were performed at the University of Neuchâtel, Switzerland. To determine bulk-rock mineralogy, an aliquot of sample (5 g) was dried at 60 °C and then ground to a homogenous powder. 800 mg of powder was pressed (20 bars) in a powder holder covered with a blotting paper. The composition of the resulting randomly oriented powder was determined by X-ray diffraction (XRD) following methods described by Ferrero (1965, 1966), Klug and Alexander (1974), and Kübler (1983) and using external standards to quantify each mineral phase. Phyllosilicate (clay minerals) content was estimated using the intensity of the $\sim 19.8^\circ$ 2θ peak and a mixed-phyllosilicates standard. Carbonate content determined by XRD was calibrated in each sample against carbonate content measured by a coulometric method (in wt.%, data from John and Mutti, 2005). XRD bulk-rock results are thus calibrated in weight percents, and values before and after calibration typically differ by $<1\%$.

Analysis of the clay mineral fraction was done using analytical procedures developed by Kübler (1987). Carbonate was removed by adding 10% HCl (1.25 N) at room temperature followed by a 3-min ultrasonic bath. Separation of different grain size fractions (clay-sized

<2μm, and fine-silt 2–16 μm) was performed by a timed settling method based on Stokes law. A drop of each fraction was then dried at room temperature onto a separate glass plate and analyzed by XRD. In order to estimate the content in smectite in the <2 μm fraction, a second analysis was made after keeping the samples overnight in an ethylene-glycol saturated atmosphere. The intensities (peak height) of selected XRD peaks characterizing each clay mineral were measured for a relative estimate of the proportion of clay minerals present. Clay mineral data are thus reported in relative percent abundance without correction factors. Where clay mineral peaks overlapped (typical for the K002/C003 peaks at ~24.5–25.2° 2θ), a mathematical profile fitting was applied using MacDiff 4.2.5. Furthermore, a zeolite "index" was estimated in each sample by using the height (in cps) of the heulandite–clinoptilolite peak at 8.96 Å and normalizing it by the sum of the heights of all clay minerals plus zeolites. This index was then multiplied by 100, and hence zeolite values are indicated here in %.

Calcite to detritus (C/D) ratios was calculated using bulk-rock X-ray diffraction results and the following formula:

$$\mathrm{C/D} = \frac{\%\mathrm{Calcite}}{(\%\mathrm{Quartz} + \%\mathrm{Phyllosilicates} + \%\mathrm{K} - \mathrm{feldspar} + \%\mathrm{Plagioclases})} \quad (1)$$

Kaolinite/micas+chlorite (K/C) ratios and kaolinite to smectite (K/S) ratios were obtained by dividing the height (in counts per second) of the 001 *hkl* peaks of the respective clays. Mass accumulation rates of phyllosilicates ($\mathrm{MAR_{Phyllosilicates}}$ in g/cm^2/ky) were calculated using the following equation:

$$\mathrm{MAR_{Phyllosilicates}} = D^{*}S_{\mathrm{Rate}}{}^{*}\%\mathrm{Phyllosilicate} \quad (2)$$

where D is the bulk dry density in g/cm^3 of the sample measured during Leg 194 (Isern et al., 2002), S_{Rate} is the sedimentation rate in cm/ky determined using the age models discussed above and %Phyllosilicates is the phyllosilicate content determined using external standard based on bulk-rock analysis. Individual accumulation rate of any particular phyllosilicate is estimated by multiplying $\mathrm{MAR_{Phyllosilicates}}$ by the relative percentage of a given clay mineral.

3. Results

3.1. Bulk-rock and clay mineral results

The minerals identified in bulk-rock analysis (Figs. 2a and 3, Table 1) are calcite (the predominant mineral), quartz, ankerite (an iron-rich dolomite), k-feldspar, plagioclases and phyllosilicates. K-feldspar and plagioclases are minor constituents of the carbonate rocks of the Marion Plateau, and the relative intensities of the XRD-peaks indicate that the plagioclase is closer to the albitic pole of the solid-solution between albite (Na-rich) and anorthite (Ca-rich). Ankerite was identified on the basis of the position of its maximum intensity peak in XRD diagrams (30.80° 2θ instead of 30.94° 2θ for dolomite). The lowest section of Hole 1192B was described as a dolomitized limestone (Isern et al., 2002), which is confirmed by the highest ankerite content documented in this study. A sharp transition from ankerite-rich intervals to non-ankerite rich interval occurs at all sites (event "AD" in Figs. 2a and 3, Table 2). Another marked decrease occurs in the phyllosilicate content towards the upper part of the three sites (event "MP" in Figs. 2a and 3, Table 2).

In the clay-sized (<2μm) and silt-sized (2–16 μm) fractions, the main clay minerals identified (Table 1) are micas, chlorite, kaolinite and smectites (Figs. 2b and 4). Mixed-layer clays of the illite–smectite type were identified in some samples but are too scarce to be quantified (<1%). Quartz, k-feldspar and plagioclases are also present in both size fractions. Additionally, zeolite (a cyclosilicate) was identified in both fractions. This zeolite was classified based on XRD diagrams as a member of the heulandite–clinoptilolite family. Heulandite–clinoptilolite content is higher in the 2–16 μm fraction (20.6% in average at Holes 1194A and 1194B, 2.7% at Hole 1192B and 34.2% at Hole 1195B) than in the <2 μm fraction (1.9% at Holes 1194A and 1194B, 0.8% at Hole 1192B and 14.0% at Hole 1195B). Trends in zeolite and other clay minerals are however consistent between the two fraction. Zeolite peaks are never visible in the bulk-rock mineralogy, indicating that its absolute abundance is low.

Based on the intensity of the 002–001–005 *hkl* peaks (Fig. 5b), the mica in both the clay-sized and fine-silt fractions was identified as a phengite with possible mixing of illite. Similarly, chlorite was characterized in a ternary plot (Fig. 5a), and results indicate that its composition oscillates between a ferromagnesian and an aluminium chlorite (Fig. 5a).

3.2. Mineralogical events and temporal trends

The onset of most of the changes recorded in the mineralogy of the Marion Plateau took place during a time-interval spanning 16.0 to 13.0 Ma (Fig. 6). Four different events can be traced between the sites investigated: a drop in ankerite content ("AD"), a minima in phyllosilicate content ("MP"), an increase in kaolinite

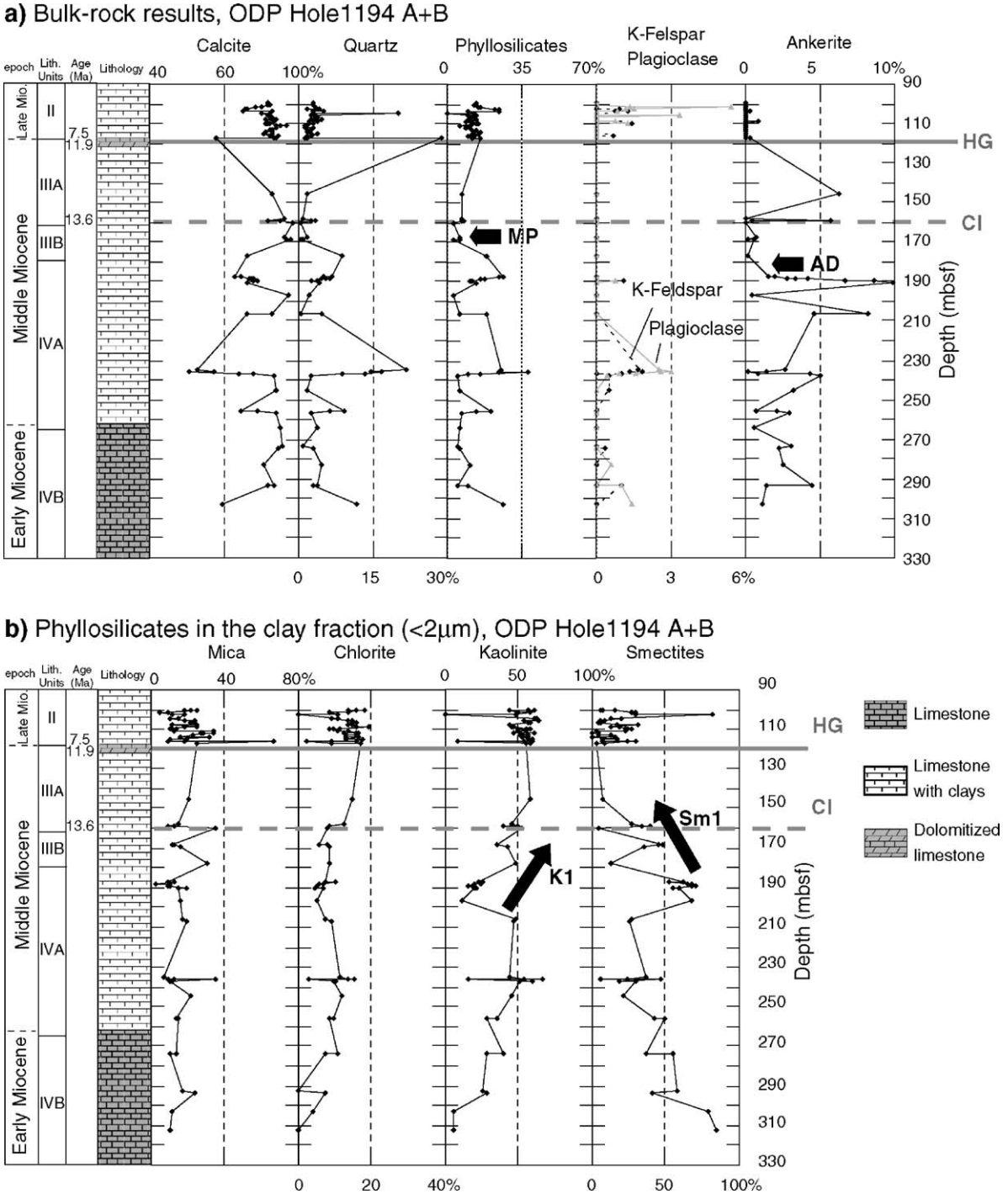

Fig. 2. X-ray results for Site 1194 (upper slope site, ~100 m water depth during the Early to Late Miocene). (a) Whole rock samples. Results are in %, calibrated using carbonate content results in wt.% published in John and Mutti (2005). CI: Condensed interval at 160 mbsf (dashed-gray line). HG: Hardground at 117.4 mbsf (solid gray line). MP: Minima in phyllosilicates. AD: Drop in ankerite content. (b) Clay fraction (<2µm). Results are in relative %, see Section 2 for details. CI: Condensed interval at 160 mbsf. HG: Hardground at 117.4 mbsf. Chl1: trend recognized in chlorite content. K1: trends recognized in kaolinite content. Sm1: trends recognized in smectite content.

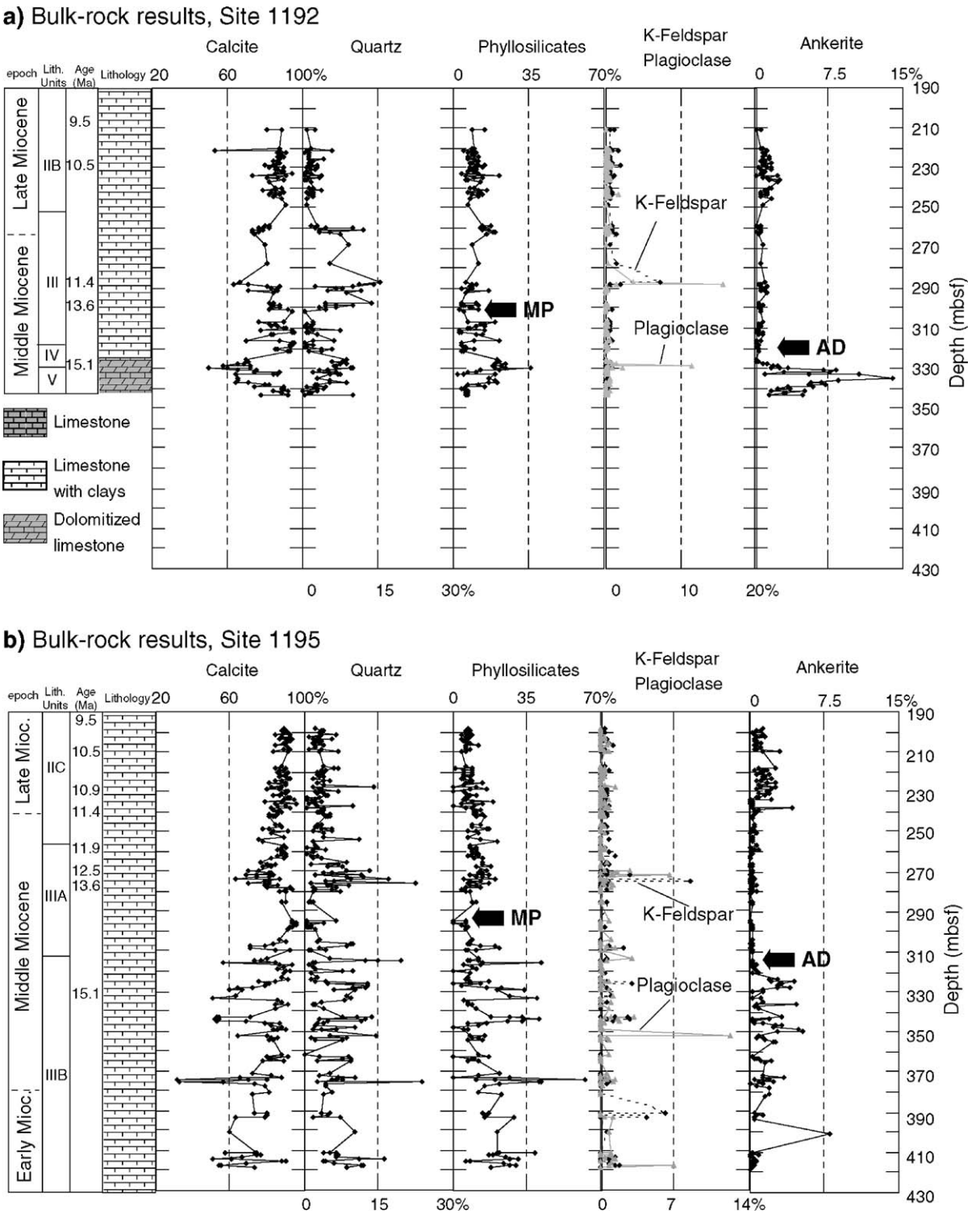

Fig. 3. X-ray results for whole rock samples from Sites 1192 (a) and 1195 (b). Both sites are distal-slope site, with ~200 m water depth during the Early to Late Miocene. Results are in % calibrated using carbonate content results in wt.% published in John and Mutti (2005). Abbreviations are as in Fig. 2.

Table 1
Average content, maxima and minima in the content of the main minerals identified in this study

	ODP Site 1194			ODP Site 1192			ODP Site 1195		
	Minima	Maxima	Average	Minima	Maxima	Average	Minima	Maxima	Average
(a) Bulk-rock results									
Calcite	40.7% (236.15 mbsf)	97.0% (160.42 mbsf)	80.9%	50.5% (330.35 mbsf)	95.4% (317.75 mbsf)	83.2%	31.2% (373.96 mbsf)	95.9% (295.93 mbsf)	81.8%
Quartz	0.2% (160.42 mbsf)	28.7% (117.41 mbsf)	4.5%	0.1% (340.95 mbsf)	15.5% (287.35 mbsf)	3.8%	0.1% (362.25 mbsf)	23.7% (375.95 mbsf)	5.0%
Phyllosilicates	0.0% (104.95 mbsf)	38.0% (236.15 mbsf)	12.6%	2.0% (333.16 mbsf)	35.5% (330.35 mbsf)	10.8%	0.0%	61.7% (373.96 mbsf)	11.7%
Ankerite	0.0%	9.9% (190.47 mbsf)	1.4%	0.2% (310.65 mbsf)	13.9% (335.40 mbsf)	1.9%	0.0%	8.0% (400.55 mbsf)	0.9%
K-feldspar	0.0%	1.8% (236.70 mbsf)	0.2%	0.0%	7.2% (287.35 mbsf)	0.5%	0.0%	8.5% (274.9 mbsf)	0.3%
Plagioclases	0.0%	3.0% (236.70 mbsf)	0.4%	0.0%	15.6% (287.85 mbsf)	0.4%	0.0%	12.4% (372.4 mbsf)	0.4%
(b) Fraction <2 μm results									
Mica	2.1% (188.05 mbsf)	66.0% (116.45 mbsf)	17.6%	3.6% (338.95 mbsf)	42.0% (342.95 mbsf)	15.1%	3.1% (344.55 mbsf)	100% (337.95 mbsf)	18.5%
Kaolinite	0.0% (102.95 mbsf)	66.5% (236.15 mbsf)	42.9%	9.4% (341.45 mbsf)	73.1% (248.82 mbsf)	42.3%	0.0%	68.0% (266.75 mbsf)	24.7%
Smectite	0.0% (111.95 mbsf)	84.7% (312.21 mbsf)	29.1%	0.0%	83.4% (338.95 mbsf)	31.1%	0.0%	94.4% (400.55 mbsf)	48.4%
Chlorite	0.0%	18.9% (108.95 mbsf)	10.4%	0.0%	26.9% (297.55 mbsf)	11.5%	0.0%	57.8% (235.85 mbsf)	8.5%

The stratigraphic depth (in mbsf) of the various events is indicated. (a) Bulk-rock fraction. (b) Clay-sized fraction (<2 μm).

content (K1) and a decrease in smectite content ("Sm1", see Table 2a and Fig. 6). The drop in ankerite and minima in phyllosilicate are used primarily for stratigraphic correlation in this paper. The oldest event is the increase in kaolinite content, which initiated around 15.6 ± 0.5 Ma at the distal slope Sites 1192 and 1195, and which is tentatively correlated with an increase around 200 mbsf at Site 1194 (with an age of 15.1 ± 1.0 Ma, Table 2a). Kaolinite content at Site 1194 is already high by 18.0 ± 1.0 Ma. The drop in ankerite content (Table 2a) does correlate between the sites with an age of 14.8 ± 0.2 Ma (Fig. 6). Even though ankerite precipitation on the Marion Plateau is a diagenetic process (Isern et al., 2002), it seems to have been coeval at all sites or to have occurred post sedimentation in identical intervals. Similarly, the initiation of the decrease in smectite (14.7 ± 0.1 Ma) and the minima in clay content (14.0 Ma) correlate well between the sites investigated (Fig. 6, Table 2a). The good coherence between the timing of these events suggests that they were probably triggered by regional changes in sedimentation patterns, continental climate, or oceanic currents.

To investigate temporal trends in mineralogy and compare our data set with other records, we calculated three indices commonly used in clay mineral studies (Robert and Chamley, 1987; Chamley et al., 1993; Adatte et al., 2002, Fig. 7, Table 2b, see Section 2): the calcite to detritus (C/D) ratios, the kaolinite to smectites (K/S) ratios and the kaolinite to micas+(K/C) ratios. The main trends in the C/D ratio at Sites 1192 and 1195 (Fig. 7a, Table 2b) is an increase of the minimal base value from 15.2 ± 0.5 Ma to $\sim 14.0 \pm 0.5$ Ma (trend CD1), followed by a decrease from 14 ± 0.5 Ma to $\sim 13.2 \pm 0.5$ Ma (trend CD2), and a final increase starting at ~13.2 Ma. No trends in C/D ratio are apparent at Site 1194, probably because the shallower water and higher-energy environment at this site tend to mechanically mix the C/D ratios, or because of the lower-resolution sampling at this site. The principal trends in K/S ratios at Sites 1192 and 1195 include an increase starting at $\sim 15.5 \pm 0.5$ Ma (trend KS1, Fig. 7b, Table 2b), followed by a plateau and a second increase starting at $\sim 13.2 \pm 0.5$ Ma (trend KS2, Fig. 7b, Table 2b). Trends in K/S ratios are somewhat similar for the proximal slope Site 1194, except that the ratio is higher than at the distal sites and the increase in K/S began earlier at this site (14.6 ± 1.0 Ma, Table 2b), though this difference could also be attributed to uncertainties in the age models. The main trends in the K/C ratios (Fig. 7c) of the distal sites are an increase in the ratio starting at 15.6 ± 0.5 Ma ("KC1", Fig. 7c,

Table 2
Description of the mineralogical event identified in the three sites investigates and their occurrence at each site (in meters below sea-floor, "mbsf")

	Event description	Site 1194	Site 1192	Site 1195
(a)	Drop in ankerite content (AD)	186.4 mbsf	327.7 mbsf	320.43 mbsf
		14.6 Ma	15.0 Ma	14.8 Ma
	Minima in Phyllosilicate content (MP)	163.4 mbsf	300.6 mbsf	294.8 mbsf
		14.0 Ma	14.0 Ma	14.0 Ma
	Increase in relative abundance of kaolinite (K1)	200.0 mbsf	329.0 mbsf	352.7 mbsf
		15.1 Ma	15.6 Ma	15.6 Ma
	Decrease in relative abundance of smectite (Sm1)	190 mbsf	320.0 mbsf	320.43 mbsf
		14.6 Ma	14.8 Ma	14.8 Ma
(b)	Increase in the calcite to detritus ratio (CD1)	–	>343.5–300.1 mbsf	418.8–294.5 mbsf
		–	>15.6–14.0	17.6–14.0 Ma
	Decrease in the calcite to detritus ratio (CD2)	–	300.1–284.6 mbsf	294.8–272.3 mbsf
		–	14.0–13.2 Ma	14.0–13.2 Ma
	Increase in the calcite to detritus ratio (CD3)	–	287 mbsf	269 mbsf
			−13.4 Ma	13.2 Ma
	Increase in the kaolinite to smectite ratio (KS1)	–	–	346.6 mbsf
		–	–	15.5 Ma
	Increase in the kaolinite to smectite ratio (KS2)	196.8 mbsf	284.6? mbsf	272.3 mbsf
		14.3? Ma	13.2? Ma	13.2 Ma
	Increase in the kaolinite to chlorite plus illite ratio (KC1)	–	>343.5 mbsf	349.8 mbsf
		–	15.6? Ma	15.6 Ma
	Increase in the kaolinite to chlorite plus illite ratio (KC2)	–	–	264 mbsf
		–	–	13.2 Ma
(c)	Increase in mass accumulation rates of kaolinite (MARK1)	–	–	352.7 mbsf
		–	–	15.6 Ma
	Increase in mass accumulation rates of kaolinite (MARK2)	–	–	272.3 mbsf
		–	–	13.2 Ma
	Decrease in mass accumulation rates of smectite (MARS1)	–	–	357.7 mbsf
		–	–	15.6 Ma

Age of the events are also indicated. (a) Relative content in clay mineral. (b) Mineral ratios based on peak height. (c) Mass accumulation rates of clays at Site 1195.

Table 2b), followed by a plateau and a second increase starting at ~12.9 ± 0.5 Ma ("KC2", Fig. 7c, Table 2b), though the timing of this second increase is harder to pinpoint. At the proximal slope Site 1194, K/C ratio remains relatively constant throughout the studied interval.

The indices discussed above are all relative, and do not reflect true fluxes (except perhaps for the C/D ratio). To circumvent this problem, we reconstructed mass accumulation rates of clays ("MAR_{clays}") at Site 1195 (Fig. 8c,d), the site with the best age model (see Section 2). By combining MAR_{clays} with the ratio discussed above, we conclude that two main phases of mineralogical changes, reflected by changes in clay fluxes (Fig. 8c,d), took place on the Marion Plateau. At ~15.6 ± 0.5 Ma, $MAR_{smectite}$ decreased ("MARS1", Table 2c, Fig. 8c) and $MAR_{kaolinite}$ increased ("MARK1", Table 2c, Fig. 8d). These changes are reflected by increases in the K/C, K/S and C/D ratio discussed above. In order to simplify further discussion we refer to this event at 15.6 Ma as Event MC1 ("mineralogical change 1"). The second phase (event MC2), centered around 13.2 Ma ± 0.5 Ma, is characterized by the onset of a second increase in $MAR_{kaolinite}$ ("MARK2", Table 2c, Fig. 8d), and again by increases in the K/C, K/S and C/D ratio as discussed above.

4. Discussion

4.1. Origin of clay minerals on the Queensland margin

The significance of the temporal trends discussed above is directly dependant on the origin and deposition history of the clay minerals. Many factors can affect the type and relative abundance of clay minerals on the shelf, including the climatic conditions under which the clays were formed, sea-level changes, current transport, reworking, marine authigenesis and diagenesis (Dixon and Weed, 1977; Chamley, 1989; Thiry, 2000). Burial diagenetic transformations for the phyllosilicates present on the Marion Plateau are unlikely because these processes generally occur at sediment depths exceeding 2 km (Chamley, 1998) and the sediments analyzed in this study have been buried under 430 m or less. Most

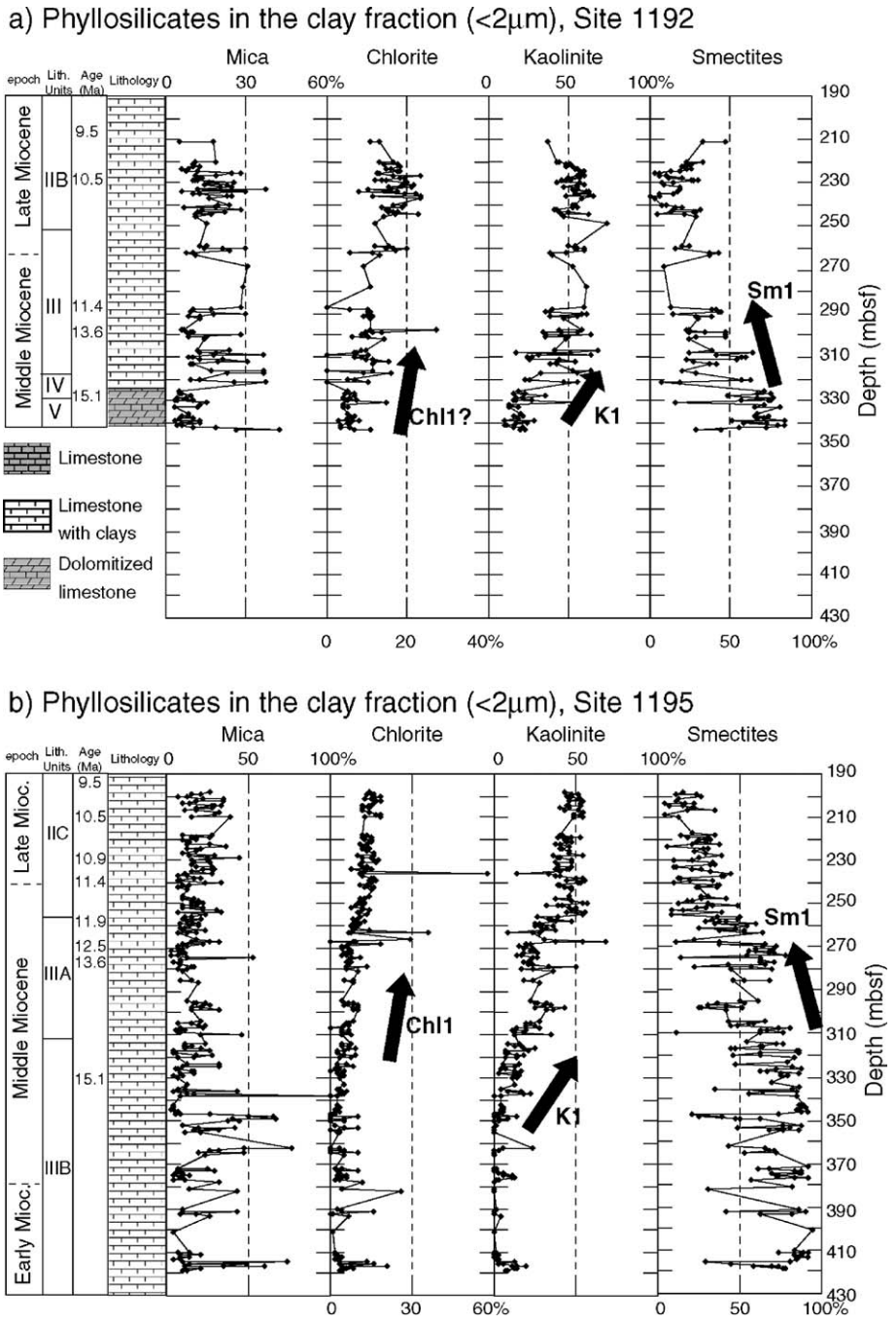

Fig. 4. X-ray results for the clay fraction (<2 µm) for samples from Sites 1192 (a) and 1195 (b). Both sites are distal-slope site, with ~200 meters water depth during the Early to Late Miocene. Results are in relative % (see Section 2). Chl1: trend recognized in chlorite content. K1: trend recognized in kaolinite content. Sm1: trends recognized in smectite content. Abbreviations are as in Fig. 2.

of the phyllosilicates and bulk minerals identified in this study have a clear continental origin. Chlorite, quartz, and feldspars prevail on the continents in areas of steep relief where active mechanical erosion limits soil formation, particularly during periods of enhanced tectonic activity, or in cold and/or desert regions where low temperatures and low rainfall reduce chemical weathering (Millot, 1970; Chamley, 1989, 1998). Phengite, the mica identified in this study, is a variety of muscovite with a silica to aluminum ratio >3

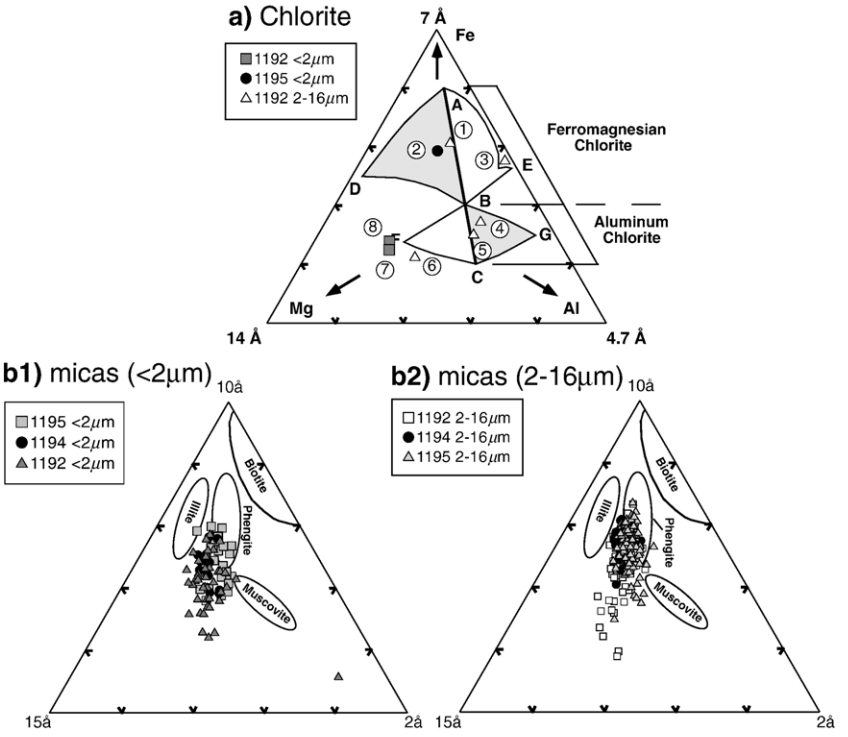

Fig. 5. (a) Ternary diagram for determination of chlorite (after Oinuma et al., 1972). Determination is made using XRD peaks at 7, 14 and 2.4 Å. Only samples with all peaks larger than 100 counts per seconds were used. (1) Sample B24043, 11.14 Ma. (2) Sample E23585, 11.35 Ma. (3) Sample B23665, 11.05 Ma. (4) Sample B25945, 11.80 Ma. (5) Sample B24004, 11.13 Ma. (6) Sample B30055, 14.03 Ma. (7) Sample B29705, 13.90 Ma. (8) Sample B25995, 11.83 Ma. (b) Ternary diagram for determination of micas in the clay fraction (<2 μm, b1) and fine silt fraction (2–16 μm, b2). Diagram is after Rey and Kübler (1983) and determination is made using XRD peaks at 10, 15 and 2 Å. Results show that in both fractions the mica is a phengite with possible admixture of illite. All diagrams plotted using ΔPlot 1.1.1 (John, 2004).

and in which Fe^{2+} and/or Mg^{2+} is substituted for Al. It is typically found in rocks that underwent high-grade metamorphism, and hence it is a good indication of a continental origin. Kaolinite, one of the two most abundant clay mineral identified in this study (as much as 50% of the clay fraction in the late middle Miocene) is also typically formed on land and is characteristic of tropical and warm-humid climatic zones with well-drained soils, accelerated leaching of the bedrock (Robert and Chamley, 1991), and minimum temperature of 15 °C (Gaucher, 1981). Though kaolinite can crystallize in permeable sandstone (Weaver, 1989), we do not consider this mechanism here because the lithologies investigated are dominantly limestones. Smectite, the second most abundant clay on the plateau, is typically formed in soils developed under a warm to temperate climate characterized by alternating humid and dry seasons (Chamley, 1998), but can also be locally formed from early diagenesis, halmirolysis (Karpoff et al., 1989) or hydrothermal weathering of volcanic rocks (Chamley, 1998). Scanning electron microscope (SEM) photographs revealed that smectite minerals present in Hole 1195B above 250 mbsf are well crystallized (Fig. 9). Smectite minerals for the interval below 250 mbsf are smaller but well-crystallized grains are also present (Fig. 9). In the intervals corresponding to smaller smectite minerals and higher relative abundance of smectite versus kaolinite, heulandite–clinoptilolite (the zeolite series identified in this study) is more abundant (below 250 mbsf at Site 1195, Fig. 10). Since heulandite–clinoptilolite and diagenetic smectite both require Si enrichments to grow (Kastner and Stonesipher, 1978), it is possible that at least a portion of the smectite below 250 mbsf has a similar origin than the zeolite. Si enrichment can be provided by opal-CT from biosiliceous sedimentation in high productivity environments, but evidence for high productivity and siliceous organisms are lacking in the Marion Plateau records. Alternatively, alteration of volcanic glass would provide the necessary material for zeolite and smectite growth (Kastner and Stonesipher, 1978). Furthermore, low k-feldspar to plagioclase ratio are associated with high zeolite content in the 2–16 μm size fraction below 250 mbsf (Fig. 10). By combining these three observations

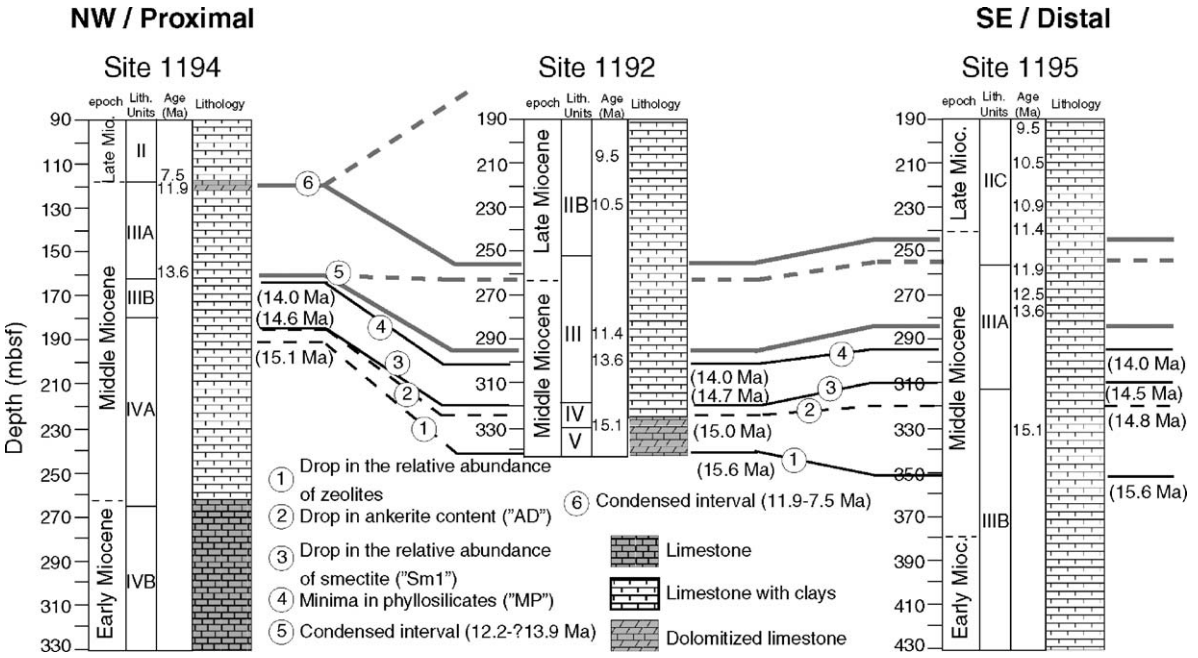

Fig. 6. Site to site correlation of events identified in clay mineral and bulk-rock mineralogy. Dating of the condensed intervals at Site 1194 and their correlation with distal sites (points 5 and 6) are from Isern et al. (2002) and John and Mutti (2005).

(variable crystallization of smectite, presence of zeolite and low k-feldspar to plagioclase ratio), we conclude that the zeolite and at least part of the smectite below 250 mbsf at Site 1195 have a volcanic origin.

Clearly, the proximity of the Australian continent and the mineral suite identified in the sediment of the plateau strongly suggests that most of the clay minerals present on the Marion Plateau have a continental origin. No data exist to constrain the exact provenance of these minerals, such as evidences of Miocene river systems and their clay mineral composition. Pinpointing the exact origin of the clays is thus difficult, but a general source area for these terrigenous minerals can be determined based on the modern and past topographical features of Northeastern Queensland (Fig. 11). One particular structural element of this region is the presence of the Great Dividing Range, a topographic barrier extending North to South across Queensland and that was a part of the landscape back in the early to middle Miocene (Grimes, 1980). The presence of the modern Great Dividing Range limits fluvial input to the location of the Marion Plateau from a narrow (~200–300 km) strip of land ranging from the eastern flank of the range to the shores of the Coral Sea. North of Cairns, rivers from the Cape York Peninsula flow North to the Gulf of Carpenteria and the Indian Ocean. West of the Great Dividing Range and South of Townsville, rivers flow in the general direction of South Australia and Lake Eyre. Past studies indicated that this flow pattern was similar in the Miocene (Fig. 11, Grimes, 1980). The proximity from land of the Townsville Trough just south of Cairns suggests that most sediment transported North of this region would have a good chance of being channelized in the Trough, and thus never reach the Marion Plateau. Finally, the general southerly direction of surface currents along the coast of Queensland (Pickard et al., 1977) suggests that sediments eroded south of the latitude of the Marion Plateau have less chances of being transported there. Accordingly, the source of terrigenous material on the plateau is inferred in this study to be east of the dividing range, south of the location of Cairns and probably directly to the east of the Marion Plateau or slightly north of the latitude of the plateau.

Within the potential source region (Fig. 11), several topographic highs composed of crystalline rocks underwent weathering in the course the Miocene and are thus considered plausible source areas for quartz, micas and feldspars, in particular Mount Tabor and Charter Towers (Vasconcelos, 1998; Li and Vasconcelos, 2002). Volcanic provinces are also abundant around Townsville (Fig. 11, after Stephenson et al., 1980), in particular the Nulla, Atherton, Mt. Fox, McBride and Wallaroo volcanic provinces. All of these volcanic terrains are likely sources for the smectite and zeolite found on the plateau. The kaolinite identified in this

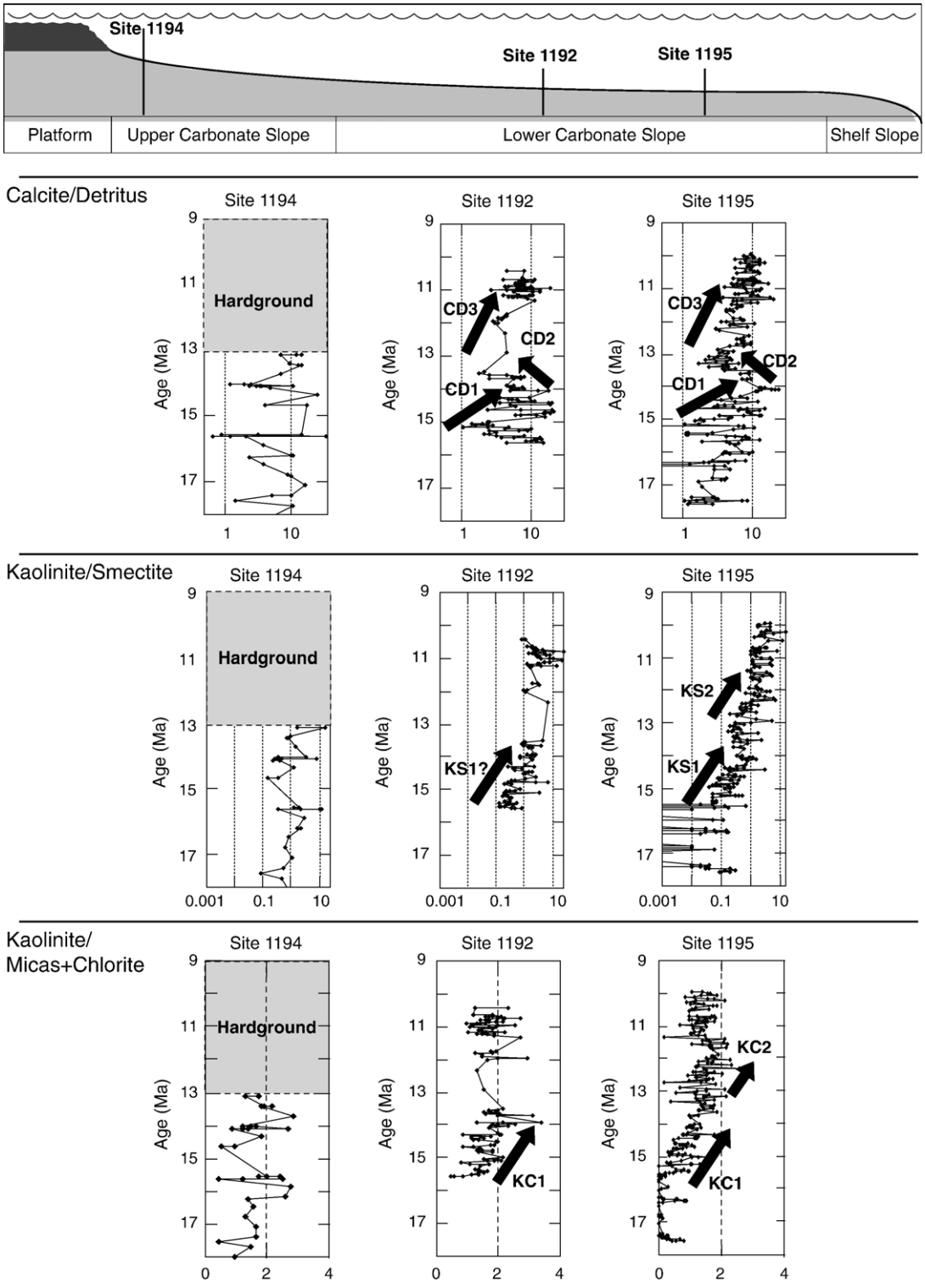

Fig. 7. Comparison of calcite to detritus, kaolinite to smecite and kaolinite to micas plus chlorite along the investigated transect. CD1,2,3: calcite to detritus trends. KS1,2: kaolinite to smectite trends. KC1,2: kaolinite to micas plus chlorite trends. Ratios have no unit, axis for CD and KS ratio are logarithmic, axis for KC ratio is linear.

study could result from the weathering under tropical conditions of both the volcanic and crystalline provinces described above, followed by river transport. However, the Australian continent is covered with thick bauxitic and kaolinitic profiles of Mesozoic to Cenozoic age, which were formed under a variety of climatic conditions, and were exposed during the Miocene (Daily et al., 1974; Anand et al., 1991; Thiry, 2000). In the early Miocene in particular, Queensland was very humid and extensive fluvio-lacustrine systems acted as traps for the kaolinite formed on land. Evidences of these systems remain in the form of kaolinite-rich formation such as the Suttor formation (Fig. 11) (Grimes, 1980; d'Auvergne, 1984), or the Duaringa basin (see Fig. 11, Grimes, 1980) south of Townsville where kaolin deposits are currently commercially exploited. Thus, sources of early Miocene kaolinite are extensive in the area investigated, and potential reworking of kaolinite and other minerals during the middle Miocene is a possibility further discussed below.

4.2. Link between clay mineral deposition on the Marion Plateau and Miocene climate change

Our data indicate that the pattern of clay mineral changes on the Marion Plateau paralleled climatic event that took place during the early to middle Miocene. The longer-term trend in clay deposition is characterized by increasing kaolinite content and decreasing smectite content. The two main stepwise increases in kaolinite input took place at ~15.6 Ma (MC1, Fig. 8) and ~13.2 Ma (MC2, Fig. 8), respectively. Both are associated with a relative increase of the C/D ratio, and thus of calcite input to the distal slope sites. The main phase of cooling and ice buildup occurred around 13.6 ± 0.5 Ma (Miller et al., 1991), suggesting that at lease the second and most dramatic change in clay mineralogy is tied to some environmental changes occurring during the middle Miocene cooling step.

A first hypothesis to link Miocene cooling with increased deposition of kaolinite on the Marion Plateau is to assume that precipitation patterns and temperature on the continent changed and favored increased rates of kaolinite formation. As stated above, kaolinite formation in soils requires significant leaching and average annual temperatures $\geq 15^{\circ}C$ (Gaucher, 1981). Increased kaolinite input at ~15.6 Ma (MC1, Fig. 8) and ~13.2 Ma (MC2, Fig. 8) could thus reflect a trend towards more "tropical" conditions in Queensland, either directly via climate change or because of the northward tectonic drift of Australia that progressively brought the continent closer to the tropical belt. To check this hypothesis, we can compare trends in clay minerals reported in this study with other continental proxies. If increased soil leaching lead to increased kaolinite formation in the course of the late early to middle Miocene, than continental proxies must show evidences of increasingly more humid conditions in Queensland. Studies of continental weathering (Li and Vasconcelos, 2002), pollen distribution (Galloway and Kemp, 1981; Kershaw et al., 1994; Macphail, 1997; Martin, 1998), and of fossil assemblages (Truswell, 1993) indicate that prior to 14.0 Ma continental climate in Queensland was warm and humid, with tropical to subtropical forests and intense chemical weathering leading to extended Mn-oxide crusts in soils (Li and Vasconcelos, 2002). However, the middle Miocene cooling that occurred around 14 Ma (McGowran and Li, 1998) induced increased aridity over the Australian continent (Stein and Robert, 1985; Martin, 1998), retraction of vegetation to the coastal areas (Truswell, 1993; Kershaw et al., 1994), and a recession of continental weathering intensity in Queensland (Li and Vasconcelos, 2002). Provided that the continental proxies are reliable, the parallel between kaolinite increase on the margin and increased aridity and cooling in Queensland is at odds with a "classical" interpretation of kaolinite as indicator of more tropical climate (Chamley, 1989; Bolle et al., 2000; Adatte et al., 2002; John

Fig. 8. Summary figure of the clay mineral evolution over the Marion Plateau and comparison with global and regional events. The gray areas mark the two main sets of event recorded in this study, MC1 at 15.6 Ma and MC2 at 13.2 Ma. (a) Summary of continental climate and weathering history as determined by other proxies. (b) Eustatic changes after Haq et al. (1987). Sea-level changes on the Marion Plateau largely reflected eustasy until around 11 Ma (dashed path), after which tectonic processed may have influenced sea-level changes. MSLF: long-term Miocene sea level fall. The lowstands identified by Betzler et al. (2000) on the Queensland Plateau are indicated at the bottom by dark boxes and the sequence boundary name (QU1, QU2, etc.). (c) Mass accumulation rates (MAR) of smectite at Site 1195, characterized by a sharp drop around 14 Ma and a steady decrease until 12 Ma. (d) Mass accumulation rates of kaolinite at Site 1195. Note the increases around 14 Ma, 12.7 Ma and 10.7 Ma. See text for discussion. (e) Kaolinite to smectite ratio for Site 588 (Stein and Robert, 1985) and Site 823 (Chamley et al., 1993) versus time. The dark line is an interpolation between data from the two sites. (f) Kaolinite to smectite ratio for Sites 1192, 1194 and 1195 versus time. The dark line is an interpolation between data from the three sites. (g) Oxygen isotope measured on benthic foraminifers (*Cibicidoides* spp.) at Sites 1192 and 1195 (John et al., 2004). "Mi3" and "Mi4" indicate the two main steps in global cooling discussed in Miller et al. (1991).

et al., 2003). Therefore, our results rule out a simple scenario where kaolinite input to the shelf is directly linked to increased precipitation on the continent.

The alternative model that we propose is that sea-level changes associated with the middle Miocene phase of global cooling played a large role in controlling clay

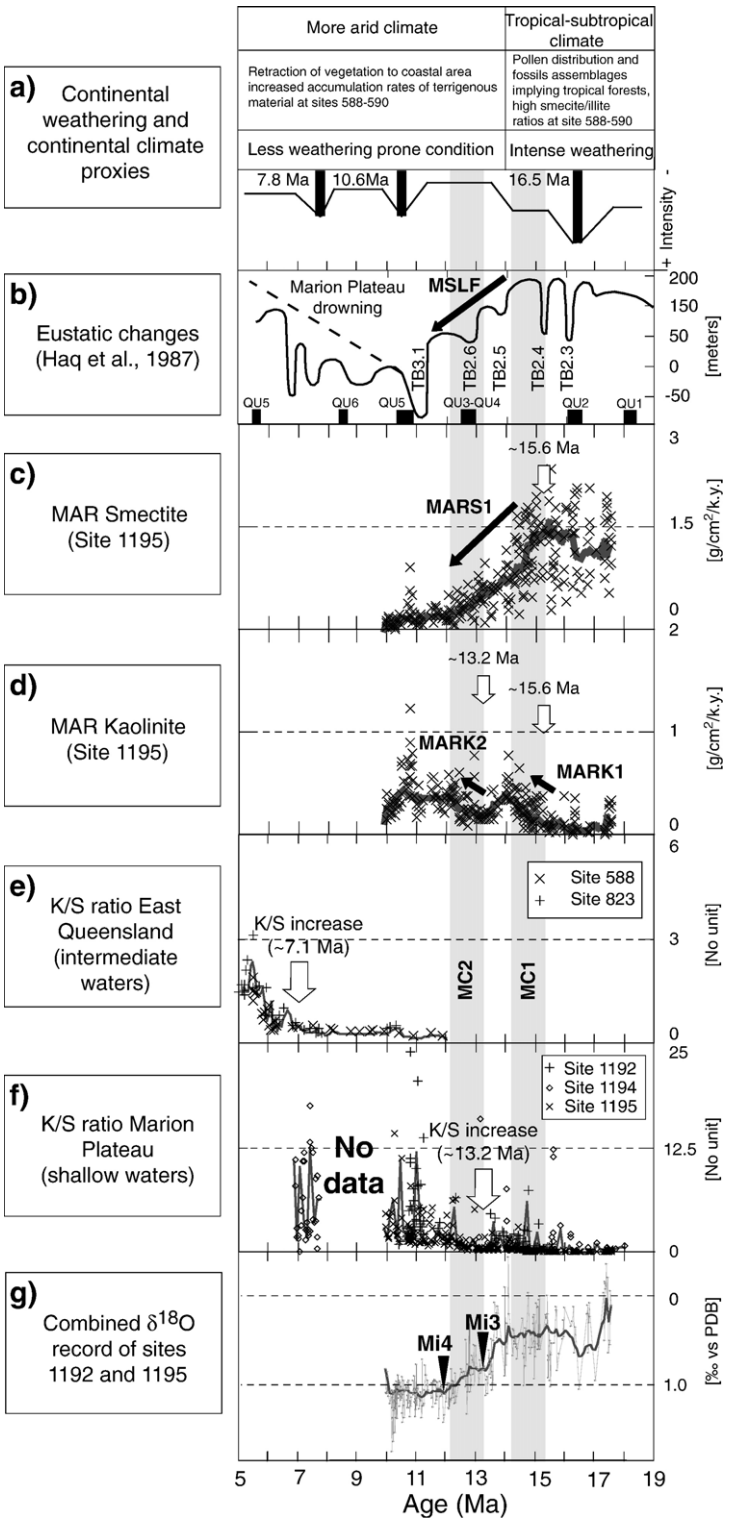

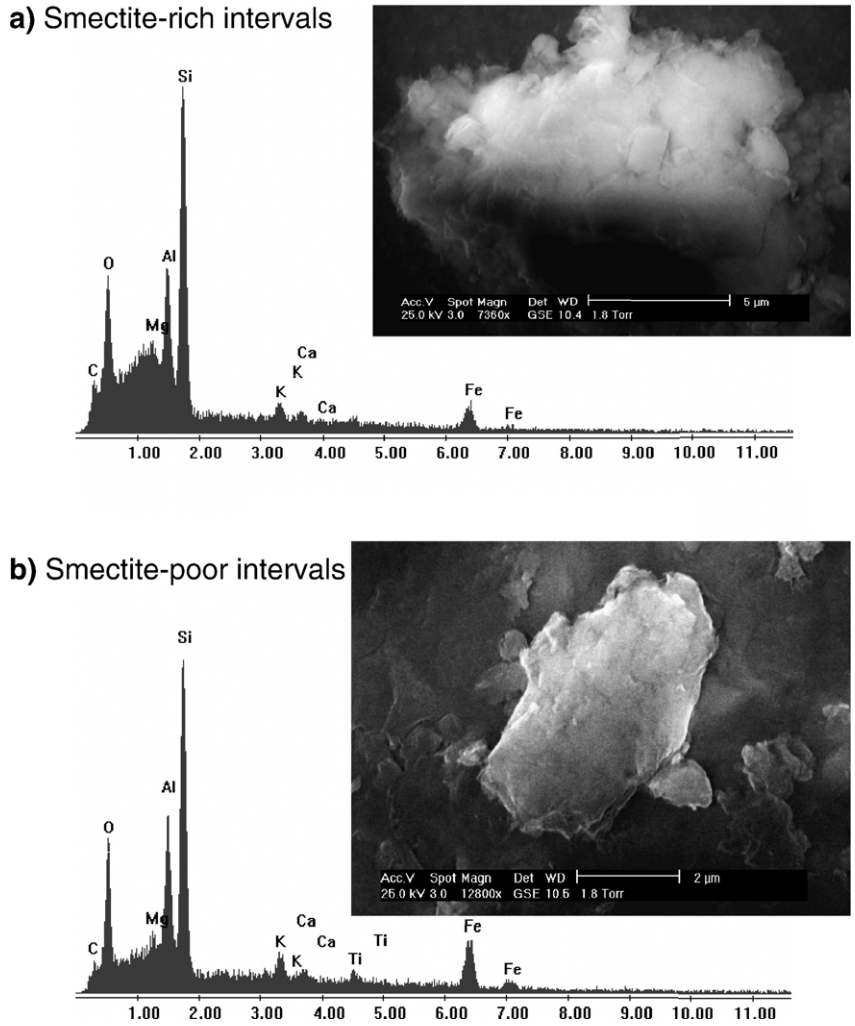

Fig. 9. Scanning electron microscope (SEM) analysis of smectite crystals in ODP Hole 1195B. (a) Interval below 250 mbsf corresponding to the interval of zeolite accumulation. Some crystal are well crystallized, indicating a continental smectite, but minor input of authigenic smectite are possible in this interval. (b) Interval above 250 mbsf, with well-crystallized minerals, probably of detritic origin.

mineral patterns on the plateau. Changes in sea level have been demonstrated by various authors to effectively impact clay mineral accumulation and kaolinite distribution in the basin (see e.g. Bolle et al., 2000; Adatte et al., 2002), and the middle Miocene is characterized by the growth of the East Antarctic Icesheet and a major sea-level fall (see John et al., 2004, and references therein). Though the exact timing of shorter terms sea-level changes on the Haq et al. (1987) curve is being increasingly questioned (see e.g. Betzler et al., 2000), there is a consensus that sea level underwent a stepwise lowering during the middle Miocene starting with sequence TB2.4 around 15.6 Ma and continuing until around 11.5 Ma (Fig. 8b) (Haq et al., 1987). The onset of the long-term sea-level fall (MSLF in Fig. 8b) occurs close to event MC1 at ~15.6 Ma, and the general duration of this fall is mirrored in the decrease in mass accumulation rates of smectite (Fig. 8c, MARS1). Lowstands were not reported on the Queensland Plateau by Betzler et al. (2000) around 15.6 Ma (Fig. 8b), but two sequence boundaries on the Great Bahamas Bank confirm that a global sea-level lowering took place around that time (Betzler et al., 2000). The second increase in kaolinite accumulation rates (MC2, Fig. 8d) occurs during a phase of pronounce sea-level falls (between 13.6 and 11.5 Ma), one of the largest sea-level fall of the early Neogene (50.0 ± 5.0 m, John et al., 2004) that was well documented on the Marion Plateau sequences (Isern et al., 2002) and the Queensland Plateau sequences (events QU3 and QU4 in Fig. 8b, after Bet-

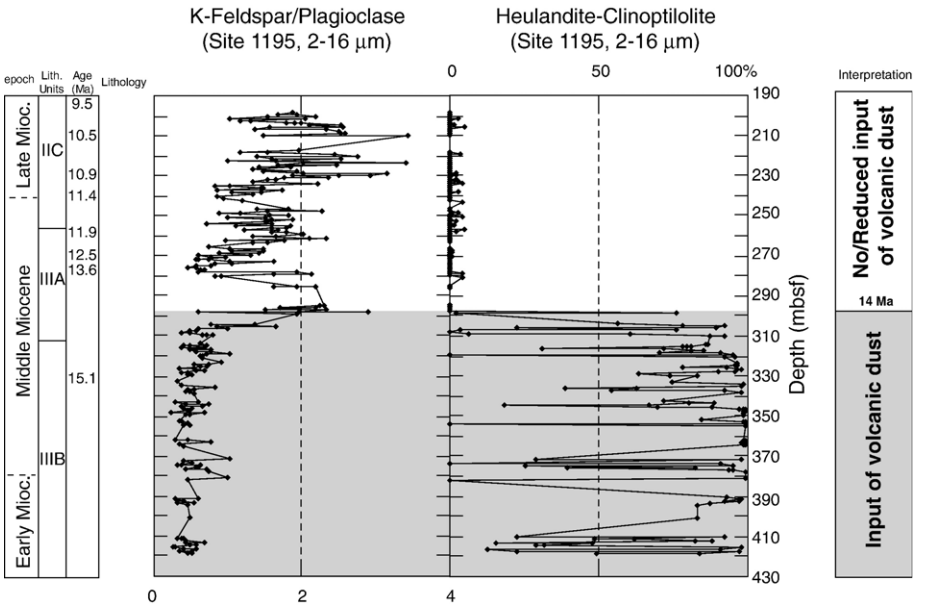

Fig. 10. Comparison between k-feldspar to plagioclase ratio (left) and occurrences of zeolite (right) at Site 1195. Both plagioclase and zeolite are high below 298 mbsf, suggesting that volcanic dust was deposited on the Marion Plateau prior to 14 Ma.

zler et al., 2000). Each of the sea-level fall described above correspond to one of the mineralogical events (MC1 and MC2), and are thus characterized by an increase of kaolinite to the distal sites and an increase of carbonate at these sites.

The parallel in the timing of long-term change in sea level and clay deposition on the plateau suggests a link between these two mechanisms. Furthermore, sea-level changes provide a simple model that can explain why higher kaolinite input and higher carbonate fluxes to the distal slope sites are associated during lowstands. Our hypothesis (illustrated in Fig. 12), based on evidences from all of the continental proxies discussed above, is that Miocene phases of cooling ("Mi" events of Miller et al., 1991) were characterized in Queensland by drier climate and lower sea level. In our model, we infer that the drier climate reduced the size of the early Miocene fluvio-lacustrine systems, thus limiting the trapping of kaolinite and providing a source of easily erodable kaolinite material in the form of ancient lacustrine sediments (such as the Suttor formation) (Fig. 12). Moreover, lower sea level during glacial periods imply a narrower shelf, and thus terrigenous material such as kaolinite can be more easily transported to the distal slope sites, hence increasing kaolinite fluxes at Sites 1192 and 1195 (Fig. 12). We explain higher carbonate to detritus ratio during lowstands by the fact that the Northern Marion and Southern Marion platforms are composed of Heterozoan carbonates (i.e. "non-tropical" carbonate). Heterozoan systems are less sensitive to changes in luminosity and have a much lower cementation potential than tropical systems (Schlager et al., 1994; James, 1997; Nelson, 2001). They thus tend to react to changes in sea level in a fashion similar to siliciclastic systems: the platform tends to aggrade when sea level is high because of the high accommodation space, retrograde when sea level rises, and prograde when sea level falls (Schlager et al., 1994; James, 1997; Nelson, 2001). Consequently, we suggest that high C/D ratios during lowstand reflect progradation of the carbonate platform towards the basin center, and consequently increased carbonate fluxes to Sites 1192 and 1195 due to the proximity of neritic carbonates. Progradation of the Marion Plateau carbonate systems during lowstands is well illustrated at Site 1194, where a lowstand ramp composed of neritic carbonates dated at ~13.6 Ma overlaps older slope sediments (Isern et al., 2002). Thus, we conclude that sea-level changes associated with drier climate and reworking of previously formed kaolinite can explain the trends in bulk and clay mineralogy reported in this study.

Alternative mechanisms potentially impacting clay deposition on the plateau exist. Oceanic currents for instance have been documented to have a distinct clay signature that could be followed for hundreds of miles in the ocean (Gingele and De Deckker, 2003; Gingele et al., 2001a,b), and thus changes in oceanic current pattern could also impact clay assemblages. Furthermore,

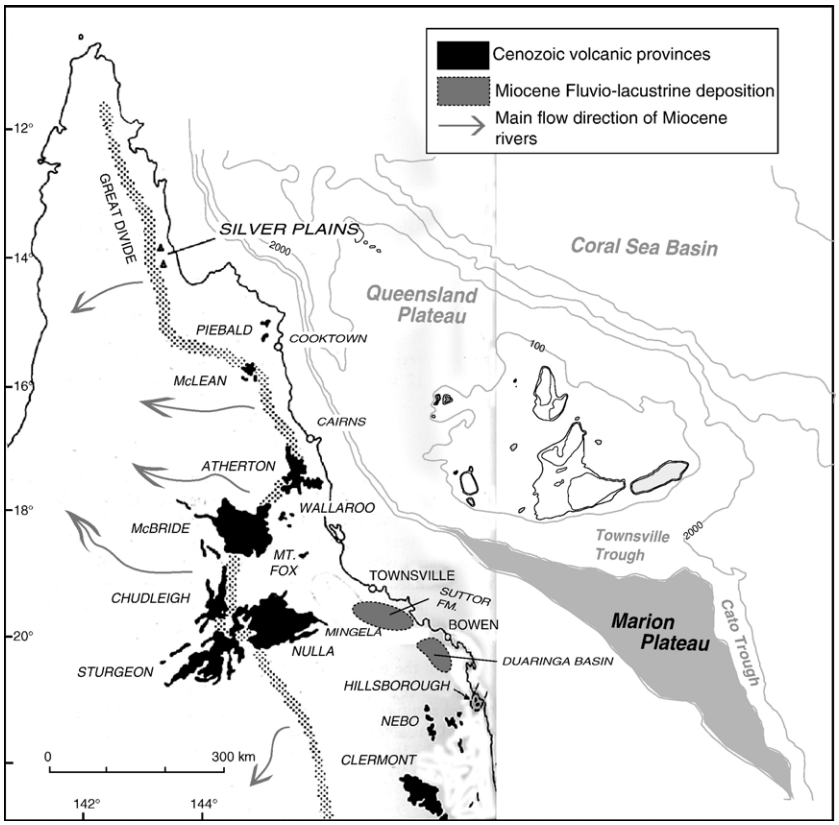

Fig. 11. Location of potential sources of sediment to the Marion Plateau. As discussed (see text), the Great Dividing Range ("Great Divide", dotted line) limits the basin for fluvial transport of material to the Marion Plateau to the east of the divide. Furthermore, the regional direction of the South Equatorial Current is indicated (Pickard et al., 1977; Tomczak and Godfrey, 1994) and the direction of this surface water current probably limits sediment input to the plateau to the Northern part of Queensland. The map and location of Cenozoic volcanic provinces are modified from Stephenson et al. (1980). Regional direction of Miocene fluvial systems and main sedimentary basin around Townsville are from Grimes (1980).

eolian transport of kaolinite could also have increased after the middle Miocene cooling step, when climate was drier. However, in the early Miocene K/S and K/C ratios are generally higher at the shallower Site 1194 than at the deeper Site 1195 (Fig. 7b,c), thus documenting a lateral distribution of kaolinite with higher kaolinite content closer to the continent. This spatial distribution is incompatible with an eolian or current transport mechanism for kaolinite, but is in good agreement with sea-level changes controlling kaolinite input to the distal locations. Moreover, neither eolian transport nor current changes can explain the correlation between high K/S and high C/D ratios, and the parallel between main phases of mineralogical changes and lowstand period. The sea-level model can easily account for these changes. For these reasons, we conclude that for the period investigated in this study sea-level changes linked with reworking of ancient kaolinite during drier periods were the main controls behind clay accumulation on the Marion Plateau.

4.3. Comparison with other regional intermediate water-depth clay records

Two other regional middle to late Miocene clay mineral records located at intermediate waters depth (~1500 m water depth) have been investigated for clay mineralogy: Site 588 (Lord Howe Rise, Stein and Robert, 1985) and Site 823 (Townsville Trough, Chamley et al., 1993). These two records only overlap with our own record over a 5 my interval between 12 and 7 Ma, and there is a 2 my gap in the Marion Plateau record. The goal of the present work is therefore not to compare these records in detail, but to contrast our finding with the conclusions of these previous studies. We note that the most prominent change in clay minerals identified at Sites 588 and 823 is an increase in the K/S ratio (Chamley et al., 1993). This change takes place around 7.1 Ma at the deeper locations (Fig. 8f). Based solely on clay mineral proxies, Chamley et al. (1993) interpreted the increase of kaolinite at Sites 588

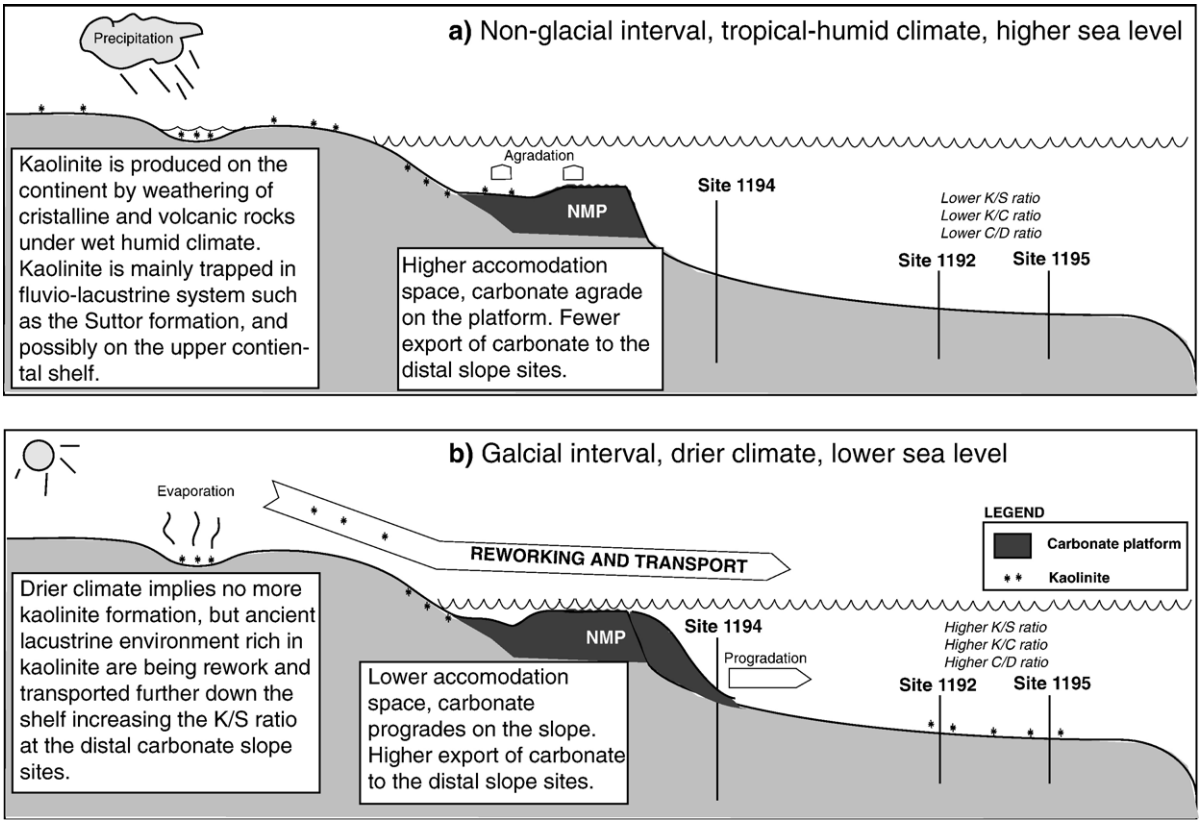

Fig. 12. Conceptual model illustrating how sea level changes linked to drier climate on the Australian continent during phases of Antarctic glaciation influenced clay and carbonate sedimentation pattern on the Marion Plateau. (a) During non-glacial interval, continental climate is more humid and kaolinite is being formed. However, due to high sea level kaolinite is mainly trapped in fluvio-lacustrine sediments and on the upper shelf. Due to the large accommodation space, carbonate platforms tend to aggrade and carbonate flux to the deeper site is more limited. (b) During glacial periods over Antarctica, sea level is lower and the climate is drier on the Australian continent. Consequently, the lacustrine systems are more restricted, kaolinite is not extensively formed but ancient lacustrine kaolinite can be more easily eroded and transported to the distal site because the shelf is narrower. Low accommodation spaces forces the platform to prograde, thus increasing carbonate flux to the distal sites.

and 823 as recording the establishment of tropical-humid conditions in Queensland, with subsequent formation and transport of kaolinite-rich soils to intermediate water-depth. The major finding of our study of the Marion Plateau sediments is that well-documented continental proxies indicate that kaolinite increases did not correlate with more humid periods during the middle Miocene, but rather corresponded to drier periods when reworking of kaolinite was more intense and sea level was lower. Hence, we caution that, though the interpretation of Chamley et al. (1993) that the northward shift of the continent induced more tropical climate in Queensland around 7.1 Ma is plausible, kaolinite accumulation offshore Australia is a complex process that does not solely depend on climate, but also largely on reworking processes. Kaolinite found offshore modern Eastern Australia largely results from reworking of ancient kaolinite-rich soils and sediments (see Thiry, 2000 and references therein), and our data suggest that a similar process was operating back in the middle Miocene (Fig. 8a).

5. Summary

Bulk-rock and clay mineral data show that although the Queensland margin was a passive margin during the Miocene, clay mineral accumulation patterns at this location were complex. Two major episodes of mineralogical changes are observed on the plateau:

- At ~15.6 Ma, the initiation of a long-term decrease in the accumulation rates of smectite is associated with a small increase in the accumulation rates of kaolinite and an increase in carbonate input to the distal sites (event MC1).
- At ~13.2 Ma, a second marked increase in accumulation of kaolinite is linked to decrease in smectite

accumulation and increase in carbonate export to the distal sites (event MC2).

We interpret both events as being mainly influenced by long-term sea-level fall coupled with increased aridity and subsequent erosion of older kaolinite-bearing lacustrine sediments. The results we have acquired for the Marion Plateau constrain the role of climate in controlling clay accumulation and weathering pattern on the Queensland margin during the middle Miocene. Global climate change did not control clay mineral deposition directly via the establishment of a tropical climate on the continent, but instead indirectly via feedbacks mechanisms involving glacio-eustasy, increased aridity and sediment reworking. Thus, our study stresses the importance of interpreting changing fluxes of kaolinite in marine settings in the light of continental proxies. This has to be taken into account when reconstructing Miocene climate changes based on the timing of export of clay minerals from the Australian continent to the deep-sea.

Acknowledgements

Samples for this study were provided by the Ocean Drilling Program (ODP). ODP is sponsored by the U.S. National Foundation (NSF) and participating countries under management of Joint Oceanographic Institutions (JOI), Inc. Funding for C. John on Leg 194 was provided by the BGR, and funding for postcruise research provided by a grant from the DFG-Schwerpunkt Program ODP (grant # MU 1680/3-1). We thank Leg 194 shipboard participants, Ivann Milenkovic for laboratory assistance with clay mineral separation, and Linda Anderson and Steve Bohaty (UCSC) who corrected a revised version of the manuscript. This paper greatly benefited from suggestions by Patrick De Deckker (editor) as well as Albert C. Hine and Christian Robert (reviewers).

References

Adatte, T., Keller, G., Stinnesbeck, W., 2002. Late Cretaceous to early Paleocene climate and sea-level fluctuations; the Tunisian record. Palaeogeography, Palaeoclimatology, Palaeoecology 178, 165–196.

Anand, R.R., Gilkes, R.J., Roach, G.I.D., 1991. Geochemical and mineralogical characteristics of bauxites Darling Range, Western Australia. Applied Geochemistry 6 (3), 233–248.

Betzler, C., Kroon, D., Reijmer, J.J.G., 2000. Synchroneity of major late Neogene sea level fluctuations and paleoceanographically controlled changes as recorded by two carbonate platforms. Paleoceanography 15 (6), 722–730.

Bolle, M.-P., Tantawy, A.A., Pardo, A., Adatte, T., Burns, S.J., Kassab, A., 2000. Climatic and environmental changes documented in the upper Paleocene to lower Eocene of Egypt. Eclogae Geologicae Helveticae 93, 33–51.

Chamley, H., 1989. Clay Mineralogy. Springer, Berlin. 623 pp.

Chamley, H., 1998. Clay mineral sedimentation in the ocean. In: Paquet, H., Clauer, N. (Eds.), Soils and Sediments (Mineralogy and Geochemistry). Springer Verlag, Berlin, pp. 269–302.

Chamley, H., Robert, C., Mueller Daniel, W., 1993. The Clay-Mineralogical Record of the Last 10 Million Years off Northeastern Australia.

d'Auvergne, P.B., 1984. Early Miocene oil shales of the Suttor Formation, Mt. Coolon District, eastern central Queensland. In: Binns, R.A. (Ed.), Geoscience in the Development of Natural Resources. Seventh Australian Geological Convention. Geological Society of Australia, Sydney, N.S.W., Australia, p. 130.

Daily, B., Twidale, C.R., Milnes, A.R., 1974. The age of the lateritized summit surface on Kangaroo Island and adjacent areas of South Australia. Journal of the Geological Society of Australia 21 (4), 387–392.

Davies, P.J., Symond, P.A., Feary, D.A., Pigram, C.J., 1989. The evolution of the carbonate platforms of Northeast Australia. In: Crevello, P.D., Wilson, J.L., Sarg, J.F., Read, J.F. (Eds.), Controls on Carbonate Platform and Basin Development. Special Publications. SEPM, Tulsa, Ok, pp. 233–258.

Derry, L.A., France–Lanord, C., 1997. Himalayan weathering and erosion fluxes; climate and tectonic controls. In: Ruddiman, W.F. (Ed.), Tectonic Uplift and Climate Change. Plenum Press, New York, pp. 289–312.

Dixon, J.B., Weed, S.B., 1977. Minerals in Soil Environments. Soil Society of America, Madison, Wisconsin. 948 pp.

Ferrero, J., 1965. Dosage des principaux minéraux des roches par diffraction de Rayon X. Rapport C.F.P. (Bordeaux), not published.

Ferrero, J., 1966. Nouvelle méthode empirique pour le dosage des minéraux par diffraction R.X. Rapport C.F.P. (Bordeaux), not published.

Flower, B.P., Kennett, J.P., 1993. Middle Miocene ocean-climate transition: high-resolution oxygen and carbon isotopic records from Deep Sea Drilling Project Site 588A Southwest Pacific. Paleoceanography 8 (6), 811–843.

Föllmi, K.B., 1996. The phosphorus cycle, phosphogenesis and marine phosphate-rich deposits. Earth-Science Reviews 40, 55–124.

Galloway, R.W., Kemp, E.M., 1981. Late Cenozoic environments in Australia. In: Keast, A. (Ed.), Ecological Biogeography of Australia. Kluwer Academic Publishers, Boston, MA, pp. 51–80.

Gaucher, G., 1981. Les Facteurs de la Pédogenèse. Dison, Belgium. 730 pp.

Gingele, F.X., De Deckker, P., 2003. Fingerprinting Australia's rivers using clays and the application for the marine record of rapid climate change. In: Roach, I.C. (Ed.), Advances in Regolith. CRC LEME, pp. 140–143.

Gingele, F.X., De Deckker, P., Hillenbrand, C.-D., 2001a. Clay mineral distribution in surface sediments between Indonesia and NW Australia—source and transport by ocean currents. Marine Geology 179.

Gingele, F.X., De Deckker, P., Hillenbrand, C.-D., 2001b. Late Quaternary fluctuations of the Leeuwin Current and palaeoclimates on the adjacent land masses: clay mineral evidence. Australian Journal of Earth Sciences 48, 867–874.

Grimes, K.G., 1980. The tertiary geology of North Queensland. In: Henderson, R.A., Stephenson, P.J. (Eds.), The Geology and Geophysics of Northeastern Australia. Geological Society of Australia Incorporated, Townsville, Australia, pp. 329–347.

Haq, B.U., Hardenbol, J., Vail, P.R., 1987. Chronology of fluctuating sea levels since the Triassic. Science 235, 1156–1167.

Hay, W.W., Soeding, E., DeConto, R.M., Wold, C.N., 2002. The Late Cenozoic uplift—climate change paradox. International Journal of Earth Sciences, 51.

Isern, A.R., Anselmetti, F.S., Blum, P., Andresen, N., Birke, T.K., Bracco Gartner, G.L., Burns, S.J., Conesa, G.A.R., Delius, H., Dugan, B., Eberli, G.P., Ehrenberg, S., Fuller, M.D., Muller, P.H., Hine, A.C., Howell, M.W., John, C.M., Karner, G.D., Kindler, P.F., Olson, B.E., Sasaki, K., Stewart, D., Wei, W., White, T.S., Wood, J.L., Yamada, T., 2002. Proceedings of the Ocean Drilling Program, Initial Reports, [CD-ROM]. Available from: Ocean Drilling Program, Texas A and M University, College Station TX 77845-9547, USA.

Jacobs, E., Weissert, H., Shields, G., Stille, P., 1996. The Monterey event in the Mediterranean: a record from the shelf sediments of Malta. Paleoceanography 11 (6), 717–728.

James, N.P., 1997. The cool-water carbonate depositional realm. In: James, N.P., Clarke, J.A.D. (Eds.), Cool-Water Carbonates. SEPM, Special Publication, vol. 56, pp. 1–20.

John, C.M., 2003. Miocene climate as recorded on slope carbonates: examples from Malta (Central Mediterranean) and Northeastern Australia (Marion Plateau, ODP LEG 194). Ph.D. Thesis, University of Potsdam, Potsdam, Germany, 90 pp. Published online at http://pub.ub.uni-potsdam.de/2003meta/0023/door.htm.

John, C.M., 2004. Plotting and analyzing data trends in ternary diagrams made easy. EOS 85 (16), 158.

John, C.M., Mutti, M., 2005. The response of heterozoan carbonate systems to Paleoceanographic, climatic and eustatic changes: a perspective from slope sediments of the Marion Plateau (ODP Leg 194). Journal of Sedimentary Research 75 (2), 51–65.

John, C.M., Mutti, M., Adatte, T., 2003. Mixed carbonate-siliciclastic record on the North African margin (Malta)—coupling of weathering processes and mid Miocene climate. GSA Bulletin 115 (2), 217–229.

John, C.M., Karner, G.D., Mutti, M., 2004. $\delta^{18}O$ and Marion Plateau backstripping: combining two approaches to constrain late middle Miocene eustatic amplitude. Geology 32 (9), 829–832.

Karpoff, A.M., Lagabrielle, Y., Boillot, G., Girardeau, J., 1989. L'authigenèse océanique de palygorskite par halmyrolyse de péridotites serpentinisées (marge de Galice); ses implications géodynamiques. Comptes Rendus de l'Académie des Sciences. Série 2, Mécanique, Physique, Chimie, Sciences de l'Univers, Sciences de la Terre 308 (7), 647–654.

Kastner, M., Stonesipher, S.A., 1978. Zeolites in pelagic sediments of the Atlantic, Pacific and Indian Oceans. In: Sand, L.B., et al. (Eds.), Natural Zeolites; Occurrence, Properties, Applications. Pergamon Press, Washington, D.C., pp. 199–221.

Kennett, J.P., 1985. The Miocene ocean. Geological Society of America Memoir 163. 337 pp.

Kershaw, A.P., Martin, H.A., McEwen Mason, J.R.C., 1994. The Neogene: a period of transition. In: Hills, R.S. (Ed.), The History of Australian Vegetation: Cretaceous to Recent. Cambridge University press, Cambridge, pp. 299–327.

Klug, H.P., Alexander, L., 1974. X-ray Diffraction Procedures for Polycrystalline and Amorphous Materials. John Wiley and Sons Inc., New York.

Kübler, B., 1983. Dosage quantitatif des minéraux majeurs des roches sédimentaires par diffraction X. Cahier de l'Institut de Géologie de Neuchâtel Série AX N0 1.1 and 12.

Kübler, B., 1987. Cristallinité de l'illite, méthodes normalisées de préparations, méthodes normalisées de mesures. Cahier Institut de Géologie de Neuchâtel Série ADX.

Li, J.-W., Vasconcelos, P., 2002. Cenozoic continental weathering and its implications for the palaeoclimate: evidence from 40Ar/39Ar geochronology of supergene K-Mn oxides in Mt. Tabor, central Queensland, Australia. Earth and Planetary Science Letters 200, 223–239.

Macphail, M.K., 1997. Late Neogene climates in Australia: fossil pollen- and spore-based estimates in retrospect and prospect. Australian Journal of Botany 45, 425–464.

Martin, H.A., 1998. The Tertiary climatic evolution and the development of aridity in Australia. Proceedings of the Linnean Society of New South Wales 119, 115–136.

McGowran, B., Li, Q.Y., 1998. Cenozoic climate change and its implications for understanding the Australian regolith. In: Eggleton, R.A. (Ed.), The State of Regolith. Geological society of Australia, Brisbane, pp. 86–103.

Miller, K.G., Feigenson, M.D., Wright, J.D., Clement, B.M., 1991. Miocene isotope reference section, Deep Sea Drilling Project Site 608; an evaluation of isotope and biostratigraphic resolution. Paleoceanography 6 (1), 33–52.

Millot, G., 1970. Geology of Clays. Springer Verlag, New York. 499 pp.

Nelson, C.S., 2001. The Cool-Water Carbonate Revolution—A New Zealand Perspective. Department of Earth Science, University of Waikato, Hamilton.

Oinuma, K., Shimoda, S., Sudo, T., 1972. Triangular diagrams of surveying chemical compositions of chlorites. Journal of Tokyo University (15), 1–13.

Pickard, G.L., Donguy, J.R., Henin, C., Rougerie, F., 1977. A review of the physical oceanography of the Great Barrier Reef and western Coral Sea. Monograph Series - Australian Institute of Marine Science 2.

Raymo, M.E., 1994. The Himalayas, organic carbon burial, and the climate in the Miocene. Paleoceanography 9 (3), 399–404.

Rey, J.-P., Kübler, B., 1983. Identification des micas des séries sédimentaires par diffraction X à partir de la série harmonique (001) des préparations orientées. Schweizerische Mineralogische und Petrographische Mitteilungen 63, 31–36.

Robert, C., Chamley, H., 1987. Cenozoic evolution of continental humidity and paleoenvironment, deduced from the kaolinite content of oceanic sediments. Palaeogeography, Palaeoclimatology, Palaeoecology 60, 171–187.

Robert, C., Chamley, H., 1991. Development of early Eocene warm climates, as inferred from clay mineral variation in oceanic sediments. Global and Planetary Change 89, 315–332.

Schlager, W., Reijmer, J.J.G., Droxler, A., 1994. Highstand shedding of carbonate platforms. Journal of Sedimentary Research B64 (3), 270–281.

Shipboard Scientific Party, 2002. Leg 194 summary. In: Isern, A.R., et al. (Eds.), Proceedings of the Ocean Drilling Program, Initial Reports, Leg, vol. 194. Ocean Drilling Program, Texas A&M University, College Station TX 77845-9547, USA, pp. 1–88. Available from:.

Stein, R., Robert, C., 1985. Siliciclastic sediments at Sites 588, 590 and 591: Neogene and Paleogene evolution in the Southwest Pacific and Australian climate. In: Kennett, J.P., von der Borch, C.C., et al. (Eds.), Initial Reports of the Deep-Sea Drilling Project. U.S. Government Printing Office, Washington.

Stephenson, P.J., Griffin, T.J., Sutherland, F.L., 1980. Cainozoic volcanism in Northeastern Australia. In: Henderson, R.A., Ste-

ani, M. (Eds.), The Geology and Geophysics of Northeastern Australia. Geological Society of Australia Incorporated, Townsville, Australia, pp. 349–374.

Struckmeyer, H.I.M., Symonds, P.A., 1997. Tectonostratigraphic evolution of the Townsville Basin, Townsville Trough, offshore northeastern Australia. Australian Journal of Earth Sciences 44, 799–817.

Thiry, M., 2000. Palaeoclimatic interpretation of clay minerals in marine deposits: an outlook from the continental origin. Earth-Science Reviews 49, 201–221.

Tomczak, M., Godfrey, S., 1994. Regional Oceanography. Pergamon Press, Oxford, U.K. 422 pp.

Truswell, E.M., 1993. Vegetation changes in the Australian Tertiary in response to climatic and phytogeographic forcing factors. Australian Systematic Botanic (6), 533–557.

Vasconcelos, P., 1998. Geochronology of weathering in Mount Isa and Charter Towers Regions, North Queensland. CRC LEME, Project 147, Brisbane, Aus.

Vincent, E., Berger, W.H., 1985. Carbon dioxide and polar cooling in the Miocene: the Monterey hypothesis. In: Sundquist, E.T., Broecker, W.S. (Eds.), Natural Variations Archean to Present. Geophysical Monograph. American Geophysical Union, pp. 455–468.

Weaver, C.E., 1989. Clays, Muds, and Shales. Developments in Sedimentology, vol. 44. Elsevier, New York. 819 pp.

Zachos, J., Pagani, M., Sloan, L., Thomas, E., Billups, K., 2001. Trends, rhythms, and aberrations in global climate 65 Ma to present. Science 292 (5517), 686–693.